Safety-critical disturbance rejection control of nonlinear systems with unmatched disturbances

Xinming Wang, *Graduate Student Member, IEEE*, Jun Yang, *Fellow, IEEE*, and Cunjia Liu, *Senior member, IEEE*, and Yunda Yan, *Member, IEEE*, and Shihua Li, *Fellow, IEEE*

***Abstract*— Safety-critical control is significant for autonomous system applications where safety is an utmost concern. Control-barrier-function (CBF)-based control has shown its promising potential and power in delivering formal safe property of dynamic nonlinear systems. The presence of disturbances, whether from matched or unmatched channels, negatively impacts CBF-based control, leading to violations of formal safety guarantees and degraded control performance. In this paper, a new safety-critical disturbance rejection control approach is proposed for nonlinear systems subject to unmatched disturbances. Owing to the naturally intractable mismatching condition, the disturbances and their high order derivatives could generate considerable negative impacts on not only the high order CBF but also the control Lyapunov function (CLF). To this end, an observer-based disturbance rejection CBF is proposed, delivering a new robust adaptive mechanism to deal with the disturbances. It is shown that by fully exploiting the disturbance estimates and adequately quantifying the impacts of estimation errors, the proposed approach provides attractive properties like formal robust safety guarantee and nominal control performance recovery under unmatched disturbances. Simulation results of path following of an unmanned aerial vehicle suffering wind disturbances verify the benefits of the proposed solution in collision avoidance and retaining nominal safety performance.**

***Index Terms*— Control barrier function, Disturbance observer, Disturbance rejection, Safety-critical control, Unmatched disturbance.**

I. Introduction

Safety guarantee has become a high priority for autonomous systems in complex environments, e.g., autonomous vehicles and intelligent robotics [1]–[4]. Among the control approaches maintaining mission-based safety constraints, control-barrier-function (CBF)-based control has emerged as a popular and effective tool for formal safety guarantee by virtue of a forward invariant set [5]. Due to its promising capability in describing complex nonlinear constraints and less computational resources in implementation, CBF-based control has made considerable progress in both theory investigation [6]–[8] and applicable case studies [9]–[11].

One of the obstacles in early CBF research is the need for precisely known system dynamics, which is usually unattainable due to external disturbances [6], [8], [12]. Clearly, ignoring the impacts of disturbances will influence the desired control performances and even degrade the formal guarantee of safety specification [13]. To address this issue, one possible treatment is to follow the philosophy of robust control theory, i.e., designing a controller such that the formal safety property is ensured even in the presence of worst-case disturbances. Toward this end, a robust CBF method is proposed in [7], where the system states are guaranteed to stay in a subset of the pre-defined safety set. This evident idea is also utilised to solve the robust safety-critical control problem of a generic dynamic robotic system with bounded uncertainties in [14]. Moreover, inspired by the input-to-state stability (ISS) [15] in nonlinear systems, the notion of input-to-state safety (ISSf) [16] is constructed based on the upper bounds of external disturbances; then an ISSf-based CBF is designed to render the system be safe within a larger invariant set compared with original one. It should be highlighted that taking the worst case of external disturbances into consideration attains strict safety constraints. However, this approach usually generates overly conservatism results in safety guarantee, which typically comes at the expense of sacrificing the control performance.

Disturbance observer-based control (DOBC) provides an alternative tool to disturbance rejection of nonlinear dynamic systems subject to disturbances [17]. By estimating and compensating for the disturbances, DOBC exhibits promising properties like strong disturbance rejection capability and nominal control performance recovery [18]. Recently, there have been some preliminary works [19]–[21] focusing on the development of robust safety-critical control using disturbance observer-assisted CBF. To be specific, by introducing the estimate of lumped disturbance into the dynamics of CBF, a modified CBF-based control approach is designed to enhance the robustness of the safety guarantee in [19]. Based on the concept of ISSfs, a tunable disturbance observer-based CBF is proposed in [20], where a new control parameter is introduced to quantify the impacts caused by the estimation error. The safety-critical control of sampled-data system with time-varying disturbance is investigated where the nonlinear disturbance observer is employed in [21]. Instead of using DO, a new robust CBF design is proposed for a disturbed system with only output measurement based on the extended state observer in [22]. In [23], when disturbances arise from a dynamically changing environment, an alternative method, i.e., the environmentally robust CBF, is developed, taking into account the upper bounds of the estimated environmental state error.

Despite the enhanced robustness of safety guarantees using observer-based CBFs as demonstrated in [19]–[23], it is important to note that these methods are limited to a class of CBFs with matched disturbances (i.e., disturbances that affect safety specifications through the same channel as the control input). It has been shown that the existence of unmatched disturbances would also generate adverse impacts on system dynamics, which will significantly degrade the control performance [24], [25]. Taking the path following of unmanned aerial vehicle (UAV) under winds as an example, the wind disturbance and its derivative will generate undesirable impacts on system dynamics via a different channel from the control input [26]. This naturally intractable mismatching condition poses great challenges for CBF-based control design as the disturbances influence the dynamics of candidate CBFs from both matched and unmatched channels. Towards this issue, in [27], the authors explore robust CBF design based on Gaussian process regression for disturbed nonlinear systems, focusing on cases where the input relative degree (IRD) and the disturbance relative degree (DRD) differ by one. Here, IRD (DRD) is defined by taking the safety specification as the interested output. This issue is further investigated in [28] by using disturbance

Xinming Wang and Shihua Li are with the Key Laboratory of Measurement and Control of CSE, Ministry of Education, School of Automation, Southeast University, Nanjing 210096, China. (email: wxm_seu@seu.edu.cn, lsh@seu.edu.cn).

Jun Yang and Cunjia Liu are with Department of Aeronautical and Automotive Engineering, Loughborough University, Loughborough LE11 3TU, UK (e-mail: j.yang3@lboro.ac.uk, c.liu5@lboro.ac.uk).

Yunda Yan is with Department of Computer Science, University College London, London, WC1E 6BT, UK (e-mail: yunda.yan@ucl.ac.uk).

observers. With the help of the disturbance observer, a preliminary result is developed for a class of single-input-single-output lower triangular nonlinear system by constructing an estimation error-based CBF in [29]. However, the analysis in [29] is restricted to a simplified scenario that considers only a single external disturbance and a specific system dynamic model. It should be highlighted that there are few works addressing the safety-critical control for a class of generalized nonlinear systems with disturbances, particularly when $\mathrm{DRD} \leq \mathrm{IRD}$.

In this paper, we propose a new safety-critical disturbance rejection control approach for a class of nonlinear systems with unmatched disturbances. To address the undesirable influences of unmatched disturbances on safety specification, disturbance observers are first introduced to obtain the estimates of disturbances and their high order derivatives. To mitigate the conservativeness arising from quantifying the estimation errors of high order disturbance derivatives, a new estimation error quantification mechanism is proposed by introducing a set of saturated disturbance estimates and their saturated estimation error bounds. Then, inspired by the design of high order CBF in [12], a disturbance rejection control barrier function (DRCBF) is constructed by fully exploiting the saturated estimates and their error bounds in each order derivatives of the DRCBF. Built upon the DRCBF, an optimisation-based control policy is proposed to achieve the strict safety task and satisfactory control performance with the support of input-to-state stable control Lyapunov function (ISS-CLF) [30]. A rigorous analysis of robust safety guarantee is established. The effectiveness of the proposed approach is verified by a practical example of UAV path following under wind disturbances. The simulation results show that the proposed control approach exhibits strict safety guarantee as well as nominal safety performance recovery.

Notations: The sets of real numbers, nonnegative real numbers and nonnegative integers are denoted as $\mathbb{R}$, $\mathbb{R}_+$ and $\mathbb{N}$. For $i, j \in \mathbb{N}$ satisfying $j \leq k$, define $\mathbb{N}_{j:k} \triangleq \{j, j+1, \cdots, k\}$ as a subset of $\mathbb{N}$. Define $\mathrm{diag}(a_1, \cdots, a_n)$ as the diagonal matrix constructed from the vector $\boldsymbol{a} = [a_1, \cdots, a_n]^T$. For a given matrix $\boldsymbol{A}$ or a vector $\boldsymbol{x}$, define the $|\boldsymbol{A}|$ or $|\boldsymbol{x}|$ as the corresponding matrix or vector with their element-wise absolute values. For any vectors $\boldsymbol{x}, \boldsymbol{y} \in \mathbb{R}^n$, $\boldsymbol{x} \leq \boldsymbol{y}$ corresponds to the element-wise inequality between vectors $\boldsymbol{x}$ and $\boldsymbol{y}$, i.e., $x_i \leq y_i, i \in \mathbb{N}_{1:n}$. Denote $\|\boldsymbol{x}\|$ as the 2-norm of vector $\boldsymbol{x}$. The saturation function $\mathrm{sat}_M(x), x \in \mathbb{R}$ with $M > 0$ is defined as $\mathrm{sat}_M(x) = x$, if $|x| < M$, and $\mathrm{sat}_M(x) = M\mathrm{sign}(x)$, if $|x| \geq M$.

II. Preliminaries and Motivation

In this section, we first cover the basic safety control design using CBF for nonlinear systems without disturbances. Then, the notions of IRD and DRD with respect to safety specifications are introduced. Finally, a UAV path following with wind disturbances is presented to highlight the challenges of ensuring safety with unmatched disturbances.

A. Safety control with CBF

Consider the following affine nonlinear system

$$\dot{\boldsymbol{x}} = \boldsymbol{f}(\boldsymbol{x}) + \boldsymbol{g}(\boldsymbol{x})\boldsymbol{u}, \tag{1}$$

where $\boldsymbol{x} \in X \subseteq \mathbb{R}^n$, $\boldsymbol{u} \in \mathbb{R}^m$, X is denoted as the admissible compact set for state. The nonlinear functions $\boldsymbol{f} : \mathbb{R}^n \to \mathbb{R}^n$, $\boldsymbol{g} : \mathbb{R}^n \to \mathbb{R}^{n\times m}$ in (1) are known locally Lipschitz functions. In the notion of CBF, a continuously differentiable function $b : \mathbb{R}^n \to \mathbb{R}$ is used to formulate the safety specification. Define $\boldsymbol{C}_0$ as the 0-superlevel set of $b(\boldsymbol{x})$,

$$\boldsymbol{C}_0 = \{\boldsymbol{x} \in \mathbb{R}^n : b(\boldsymbol{x}) \geq 0\}, \tag{2}$$

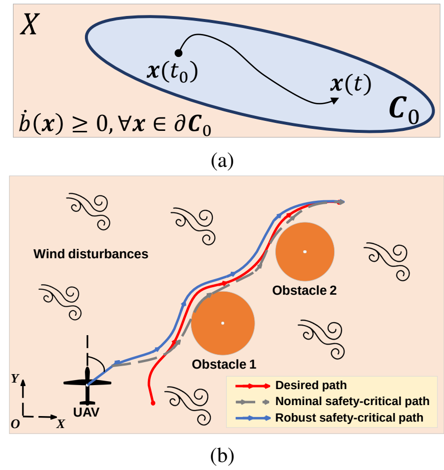

Fig. 1: Illustration of the concept of CBF and the safety-critical path following of UAV with wind disturbances and obstacles: (a) Under the control action from K_{CBF}, the trajectory $\boldsymbol{x}(t) \in \boldsymbol{C}_0$, $\forall t \geq 0$, if $\boldsymbol{x}(0) \in \boldsymbol{C}_0$; (b) In the presence of wind disturbances, the conventional controller may lead to collisions.

and $\partial\boldsymbol{C}_0 \triangleq \{\boldsymbol{x} \in \mathbb{R}^n : b(\boldsymbol{x}) = 0\}$ is the boundary, and $\mathrm{Int}(\boldsymbol{C}_0) \triangleq \{\boldsymbol{x} \in \mathbb{R}^n : b(\boldsymbol{x}) > 0\}$ is the non-empty interior. The system (1) is *safe* with respect to the set $\boldsymbol{C}_0$, if there exists a control action $\boldsymbol{u}$ renders the set $\boldsymbol{C}_0$ forward invariant, i.e., for each initial state $\boldsymbol{x}(0) \in \boldsymbol{C}_0$, $\boldsymbol{x}(t) \in \boldsymbol{C}_0$, $\forall t > 0$. Then, the CBF is defined as follows

Definition *1 ([5]):* Considering the system (1), a continuously differentiable function $b : \mathbb{R}^n \to \mathbb{R}$ is a CBF, if there exists a positive constant k_0 subject to

$$\sup_{\boldsymbol{u}\in\mathbb{R}^m} \left\{ L_{\boldsymbol{f}} b(\boldsymbol{x}) + L_{\boldsymbol{g}} b(\boldsymbol{x})\boldsymbol{u} + k_0 b(\boldsymbol{x}) \right\} \geq 0,\ \forall \boldsymbol{x} \in X, \tag{3}$$

where $L_{\boldsymbol{f}}$, $L_{\boldsymbol{g}}$ are standard Lie derivatives along $\boldsymbol{f}(\boldsymbol{x})$ and $\boldsymbol{g}(\boldsymbol{x})$.

Given a valid CBF $b(\boldsymbol{x})$, if the initial states of system satisfy $\boldsymbol{x}(0) \in \boldsymbol{C}_0$, then any Lipschitz continuous controller $\boldsymbol{u}(\boldsymbol{x})$ belonging to $K_{\mathrm{CBF}} \triangleq \{\boldsymbol{u} \in \mathbb{R}^m | L_{\boldsymbol{f}} b(\boldsymbol{x}) + L_{\boldsymbol{g}} b(\boldsymbol{x})\boldsymbol{u} \geq -k_0 b(\boldsymbol{x})\}$ renders the system (1) safe. The typical trajectory of system (1) satisfying (3) is presented in Fig. 1 (a).

B. System with unmatched disturbances

The considered nonlinear system (1) subject to external disturbances $\boldsymbol{d}$ can be expressed as follows

$$\dot{\boldsymbol{x}} = \boldsymbol{f}(\boldsymbol{x}) + \boldsymbol{g}(\boldsymbol{x})\boldsymbol{u} + \boldsymbol{d}, \tag{4}$$

where $\boldsymbol{d} = [d_1, d_2, \ldots, d_n]^T$ are external disturbances. Define the smooth function $h : \mathbb{R}^n \to \mathbb{R}$ as an output characterizing safety specification of system (4). When dealing with unmatched disturbances like system (4), it is generally infeasible to completely reject their effects [31]. However, it is possible to remove the influence of disturbances from the $h(\boldsymbol{x})$ [25]. Without loss of generality, it is supposed that the equilibrium $\boldsymbol{x}_0$ of the system (4) without the disturbances is the origin. The IRD to $h(\boldsymbol{x})$ is defined as follows:

Definition *2 ([31]):* The relative degree from the control inputs to the output $h(\boldsymbol{x})$ is r_I at the equilibrium $\boldsymbol{x}_0$ if $L_{\boldsymbol{g}_j} L_{\boldsymbol{f}}^k = 0$ $(1 \leq j \leq m)$ for all $k < r_I - 1$ for all $\boldsymbol{x}$ in a neighborhood of $\boldsymbol{x}_0$, the vector $\boldsymbol{A}(\boldsymbol{x}) = [L_{\boldsymbol{g}_1} L_{\boldsymbol{f}}^{r_I-1}, L_{\boldsymbol{g}_2} L_{\boldsymbol{f}}^{r_I-1}, \ldots, L_{\boldsymbol{g}_m} L_{\boldsymbol{f}}^{r_I-1}]^T$ has at least one non-zero element. Here $\boldsymbol{g}_j$ is the jth row vector of $\boldsymbol{g}(\boldsymbol{x})$.

Similarly, the DRD to $h(\boldsymbol{x})$ at $\boldsymbol{x}_0$ can be defined as r_D. It should be noted that the CBF introduced above is an artificial output defined to characterise the safety specification [32]. Thus, the CBF design for the disturbed system (4) should account for the relationships between IRD and DRD. The following example illustrates this point further.

C. A motivating example: path following of UAV

Consider the collision-avoidance path following of UAV in the horizontal plane as illustrated by Fig. 1 (b), where (x_p^s, y_p^s) and (x_p^f, y_p^f) are the start and end path points, respectively. In Fig. 1 (b), the desired path is shown as a red solid line. The standard safety-critical path, generated by a conventional CBF-CLF-based controller, is the gray dashed line. The robust safety-critical path, accounting for obstacles and winds, is represented by a blue solid line.

The kinematics of the UAV can be expressed as follows [33]

$$\begin{aligned} &\dot{p}_x = V_a \cos\psi + d_x,\ \dot{p}_y = V_a \sin\psi + d_y, \\ &\dot{\psi} = u_\psi, \end{aligned} \tag{5}$$

where p_x, p_y are the position of UAV in the inertial frame, V_a represents its airspeed, ψ is the heading angle, u_ψ is the equivalent control input driving the direction of UAV, and d_x, d_y are the wind disturbances. In this case, the UAV is required to follow a desired path while keeping a safe distance from some obstacles $O_i, i \in \mathbb{N}$. Despite the path following task, the safety concern of obstacles is the high priority of the mission. We can use the candidate CBFs $b_i(p_x, p_y) = (p_x - x_{o,i})^2 + (p_y - y_{o,i})^2 - R_{o,i}^2$ to interpret such safety specifications, where $x_{o,i}, y_{o,i}$ is the ith position of obstacle's center and $R_{o,i}$ is its radius. To achieve the critical safety task, a control policy should be designed to maintain the positiveness of $b_i(p_x(t), p_y(t)), \forall t > 0$ when $b_i(p_x(0), p_y(0)) \geq 0$ in the sense of CBF-based safety control. Then, its time derivatives along the system (5) are

$$\begin{aligned} \dot{b}_i(p_x, p_y) =& 2V_a[(p_x - x_{o,i})\cos\psi + (p_y - y_{o,i})\sin\psi] \\ &+ 2(p_x - x_{o,i})d_x + 2(p_y - y_{o,i})d_y, \\ \ddot{b}_i(p_x, p_y) =& 2V_a^2 + 2d_x^2 + 2d_y^2 + 2(p_x - x_{o,i})\dot{d}_x + 2(p_y - y_{o,i}) \\ &\dot{d}_y + 2V_a[(p_y - y_{o,i})\cos\psi - (p_x - x_{o,i})\sin\psi]u_\psi \\ &+ 4V_a(d_x\cos\psi + d_y\sin\psi). \end{aligned} \tag{6}$$

Following from (6), it is evident that the DRD r_D to $b_i(p_x, p_y)$ is less than the IRD r_I. This indicates that the wind disturbances d_x, d_y and their derivatives not only pollute the $b_i(p_x, p_y)$ via matched channel but also alter its behavior from the unmatched channel, which can not be solved by the current CBF-based control approaches. Especially, the existences of $2(p_x - x_{o,i})d_x$ and $2(p_y - y_{o,i})d_y$ increase the difficulty in design and analysis of robust CBF. This motivates us to design a new CBF to actively reject the impacts on safety performance caused by unmatched disturbances.

III. Robust Safety Control Design with Unmatched Disturbances

In this section, we will show the proposed robust safety control solution under unmatched disturbances. Denote the $b(\boldsymbol{x})$ as the candidate safe function for disturbed nonlinear system (4). To reduce the complexity in analysis, we assume the external disturbances do not change the control relative degree $r \in \mathbb{N}$ of $b(\boldsymbol{x})$, and suppose the high order derivatives of $b(\boldsymbol{x})$ can be expressed as follows

$$\begin{aligned} &b^{(i)}(\boldsymbol{x}) = \alpha_i(\boldsymbol{x}) + \beta_i(\boldsymbol{x}, \boldsymbol{d}, \dot{\boldsymbol{d}}, \ldots, \boldsymbol{d}^{(i-1)}), i \in \mathbb{N}_{1:r-1}, \\ &b^{(r)}(\boldsymbol{x}) = \alpha_r(\boldsymbol{x}) + \boldsymbol{\beta}_u(\boldsymbol{x})\boldsymbol{u} + \beta_r(\boldsymbol{x}, \boldsymbol{d}, \dot{\boldsymbol{d}}, \ldots, \boldsymbol{d}^{(r-1)}), \end{aligned} \tag{7}$$

where $\alpha_i : \mathbb{R}^n \to \mathbb{R}$, $\beta_i : \mathbb{R}^n \times \bar{\mathbb{D}}_{i-1} \to \mathbb{R}$, in which $\bar{\mathbb{D}}_{i-1} \triangleq \mathbb{D}_0 \times \mathbb{D}_1 \times \cdots \times \mathbb{D}_{i-1}$, and $\boldsymbol{\beta}_u : \mathbb{R}^n \to \mathbb{R}^m$ is a $1 \times m$ raw vector satisfying $\boldsymbol{\beta}_u(\boldsymbol{x}) \neq 0, \forall \boldsymbol{x} \in X$. The sets $\mathbb{D}_i,\ i \in \mathbb{N}_{0:r-1}$ are denoted as the compact sets of external disturbance vector $\boldsymbol{d}$ and their derivatives $\boldsymbol{d}^{(i)}$. It is important to mention that a large number of nonlinear systems meet the condition stated in (7), e.g., the single-input-single-output lower triangular nonlinear systems.

The external disturbances d_i considered in this paper are assumed to satisfy the following assumption.

Assumption *1:* The disturbances $d_i, i \in \mathbb{N}_{1:n}$ are differentiable and there exists a set of known positive real numbers $\delta_{i,j} \in \mathbb{R}_+, j \in \mathbb{N}_{0:n}$ that $|d_i^{(j)}(t)| \leq \delta_{i,j}, \forall t \geq 0$.

Remark *1:* The disturbances considered in this study encompass most of the common types that occur in various systems, such as constant, sinusoidal and polynomial signals.

The nonlinear functions $\beta_i(\boldsymbol{x}, \boldsymbol{d}, \dot{\boldsymbol{d}}, \cdots, \boldsymbol{d}^{(i-1)}), i \in \mathbb{N}_{1:r}$ are also supposed to satisfy the following assumption.

Assumption *2:* There exist known strictly increasing positive functions $\gamma_i(\boldsymbol{x})$ and $\tilde{\gamma}_i(\boldsymbol{y}), i \in \mathbb{N}_{1:r}$ such that for all $\boldsymbol{x} \in X$, $\boldsymbol{y}_j, \hat{\boldsymbol{y}}_j \in \bar{\mathbb{D}}_j, j \in \mathbb{N}_{0:i-1}$, the following inequalities hold

$$\begin{aligned} |\beta_i(\boldsymbol{x}, \boldsymbol{y}_0, \ldots, \boldsymbol{y}_{j-1}) - \beta_i(\boldsymbol{x}, \hat{\boldsymbol{y}}_0, \ldots, \hat{\boldsymbol{y}}_{j-1})| \leq \gamma_i(\boldsymbol{x})\tilde{\gamma}_i([\tilde{\boldsymbol{y}}_0^T, \\ \tilde{\boldsymbol{y}}_1^T, \ldots, \tilde{\boldsymbol{y}}_{j-1}^T]^T), \end{aligned} \tag{8}$$

where $\tilde{\boldsymbol{y}}_j = \boldsymbol{y}_j - \hat{\boldsymbol{y}}_j$.

Remark *2:* Due to the wide range of mission-based safety specifications described by $b(\boldsymbol{x})$, exhibiting a uniform formulation of $\beta_i(\boldsymbol{x}, \boldsymbol{d}, \dot{\boldsymbol{d}}, \ldots, \boldsymbol{d}^{(i-1)})$ is a difficult task. To reduce the complexity and present the key idea of rejecting unmatched disturbances, the above Assumption is made. Actually, the nonlinear functions $\beta_i(\boldsymbol{x}, \boldsymbol{d}, \dot{\boldsymbol{d}}, \ldots, \boldsymbol{d}^{(i-1)})$ satisfying Assumption 2 enclose a large set of possible nonlinear functions of disturbances, e.g., d_1^2 and $d_1 d_2$. For d_1^2, it is obtained that $d_1^2 - \hat{d}_1^2 = (d_1 + \hat{d}_1)(d_1 - \hat{d}_1) \leq 2\max\{\bar{d}_1, |\hat{d}_1|\}|d_1 - \hat{d}_1|$; for $d_1 d_2$, it is obtained that $d_1 d_2 - \hat{d}_1 \hat{d}_2 = d_1 d_2 - d_1 \hat{d}_2 + d_1 \hat{d}_2 - \hat{d}_1 \hat{d}_2 \leq 2\max\{\bar{d}_1, |\hat{d}_2|\}\sqrt{(d_1 - \hat{d}_1)^2 + (d_2 - \hat{d}_2)^2}$.

In the following, we will first introduce the design of disturbance observers and the corresponding quantification mechanism of the estimation errors. With those in mind, the proposed DRCBF is designed under unmatched disturbances. Finally, an optimisation-based robust control policy is formulated by integrating with the technique of ISS-CLF.

A. Disturbance observer design and estimation error quantification

Considering the system (4), the disturbance observers employed from [34] are constructed as follows

$$\begin{aligned} &\dot{\boldsymbol{\xi}}_i = \boldsymbol{A}(\boldsymbol{\xi}_i + \boldsymbol{L}_i x_i) - \boldsymbol{L}_i[f_i(\boldsymbol{x}) + g_i(\boldsymbol{x}, \boldsymbol{u}) + \boldsymbol{C}(\boldsymbol{\xi}_i + \boldsymbol{L}_i x_i)], \\ &\hat{\boldsymbol{w}}_i = \boldsymbol{\xi}_i + \boldsymbol{L}_i x_i. \end{aligned} \tag{9}$$

where $f_i(\boldsymbol{x})$, $g_i(\boldsymbol{x}, \boldsymbol{u})$ are the i-th component of $\boldsymbol{f}(\boldsymbol{x})$ and $\boldsymbol{g}(\boldsymbol{x})\boldsymbol{u}$, $\boldsymbol{\xi}_i \in \mathbb{R}^n$ is the auxiliary state, $\boldsymbol{A} = \begin{bmatrix} \boldsymbol{0} & \boldsymbol{I}_{n-1} \\ 0 & \boldsymbol{0} \end{bmatrix}$, $\boldsymbol{C} = [1, 0, \ldots, 0]$, and $\boldsymbol{L}_i \in \mathbb{R}^{n \times 1}$ is the parameter vector to be designed.

Denote $\hat{\boldsymbol{w}}_i = [\hat{w}_{i,0}, \hat{w}_{i,1}, \ldots, \hat{w}_{i,n-1}]^T$ as the estimate vector of disturbance d_i and its time-derivatives, and define the estimation error $\boldsymbol{e}_i = \boldsymbol{w}_i - \hat{\boldsymbol{w}}_i$, where $\boldsymbol{w}_i \triangleq [d_i, \dot{d}_i, \ldots, d_i^{(n-1)}]^T$. Combining (4) and (9), its dynamics is expressed as

$$\dot{\boldsymbol{e}}_i = \bar{\boldsymbol{A}}_i \boldsymbol{e}_i + \boldsymbol{\sigma}_i, \tag{10}$$

where $\bar{\boldsymbol{A}}_i = \boldsymbol{A} - \boldsymbol{L}_i \boldsymbol{C}$ and $\boldsymbol{\sigma}_i = [0, 0, \ldots, d_i^{(n)}]^T$. By selecting a proper gain matrix $\boldsymbol{L}_i$, the $\bar{\boldsymbol{A}}_i$ is Hurwitz. Then, the system (10) is input-to-state stable with respect to the $\boldsymbol{\sigma}_i$ under Assumption 1.

Assuming the $\bar{\boldsymbol{A}}_i$ has n independent eigenvalues $\lambda_{i,j}, j \in \mathbb{N}_{1:n}$, there exists an invertible matrix $\boldsymbol{P}_i$ such that $\boldsymbol{P}_i^{-1}\bar{\boldsymbol{A}}_i\boldsymbol{P}_i = \boldsymbol{\Lambda}_i$ with $\boldsymbol{\Lambda}_i \triangleq \mathrm{diag}(\lambda_{i,1}, \ldots, \lambda_{i,n})$. Moreover, by setting zero initial condition of $\hat{\boldsymbol{w}}_i(0)$ and considering Assumption 1, its solution can be overestimated by the following estimation error bound $\boldsymbol{\varepsilon}_i(t)$

$$\begin{aligned}
|\boldsymbol{e}_i(t)| \leq& |e^{\bar{\boldsymbol{A}}_i t}\boldsymbol{e}_i(0) + \int_0^t e^{\bar{\boldsymbol{A}}_i(t-\tau)}\boldsymbol{\sigma}_i(\tau)\mathrm{d}\tau| \\
\leq& |\boldsymbol{P}_i e^{\boldsymbol{\Lambda}_i t}\boldsymbol{P}_i^{-1}|\bar{\boldsymbol{\delta}}_i(0) + |\boldsymbol{P}_i|\int_0^t |e^{\boldsymbol{\Lambda}_i(t-\tau)}|\mathrm{d}\tau|\boldsymbol{P}_i^{-1}|\bar{\boldsymbol{\delta}}_{i,\sigma} \\
=& |\boldsymbol{P}_i e^{\boldsymbol{\Lambda}_i t}\boldsymbol{P}_i^{-1}|\bar{\boldsymbol{\delta}}_i(0) - |\boldsymbol{P}_i||\boldsymbol{\Lambda}_i^{-1}e^{\boldsymbol{\Lambda}_i t}||\boldsymbol{P}_i^{-1}|\bar{\boldsymbol{\delta}}_{i,\sigma} \\
&+ |\boldsymbol{P}_i||\boldsymbol{\Lambda}_i^{-1}||\boldsymbol{P}_i^{-1}|\bar{\boldsymbol{\delta}}_{i,\sigma} \\
\triangleq& \boldsymbol{\varepsilon}_i(t).
\end{aligned} \tag{11}$$

where $\bar{\boldsymbol{\delta}}_i(0) = [\delta_{i,0}, \delta_{i,1}, \ldots, \delta_{i,n-1}]^T$ and $\bar{\boldsymbol{\delta}}_{i,\sigma} = [0, \ldots, \delta_{i,n}]^T$. It should be noted that the error quantification proposed in (11) will unavoidably experience a dramatic change in the transient phase since the high order derivatives of the disturbance d_i are required to be estimated. To address this issue, the following new error quantification mechanism is proposed. Based on Assumption 1, we first define the following saturated disturbance estimates

$$\hat{w}_{i,j}^{\mathrm{sat}} = \mathrm{sat}_{\delta_{i,j}}(\hat{w}_{i,j}), \tag{12}$$

where $i \in \mathbb{N}_{1:n},\ j \in \mathbb{N}_{0:n-1}$. With (11) in mind, we further define the following saturated estimation error bounds

$$\varepsilon_{i,j}^{\mathrm{sat}} = \mathrm{sat}_{2\delta_{i,j}}(\varepsilon_{i,j}), \tag{13}$$

where $\varepsilon_{i,j}$ is the corresponding component of the error bound vector $\boldsymbol{\varepsilon}_i$. The following theorem is concluded to show the elegant properties of the proposed error quantification approach.

Theorem *1:* Under Assumption 1, if the $\bar{\boldsymbol{A}}_i$ is Hurwitz with n independent eigenvalues, then the errors between $d_i^{(j)}, i \in \mathbb{N}_{1:n},\ j \in \mathbb{N}_{0:n-1}$ and the saturated estimates $\hat{w}_{i,j}^{\mathrm{sat}}$ satisfy $|d_i^{(j)} - \hat{w}_{i,j}^{\mathrm{sat}}| \leq \varepsilon_{i,j}^{\mathrm{sat}}$.

Proof: In the following, we will demonstrate that the saturated estimation error bound (13) is able to quantify the difference between $d_i^{(j)}$ and the saturated estimates $\hat{w}_{i,j}^{\mathrm{sat}}$.

Under Assumption 1, it is clear that $|d_i^{(j)} - \hat{w}_{i,j}^{\mathrm{sat}}| \leq 2\delta_{i,j}$. If $|e_{i,j}| > 2\delta_{i,j}$, due to the fact that $\varepsilon_{i,j} \geq e_{i,j}$, it is obtained that $\varepsilon_{i,j}^{\mathrm{sat}} = 2\delta_{i,j}$. Then, we have $|d_i^{(j)} - \hat{w}_{i,j}^{\mathrm{sat}}| \leq \varepsilon_{i,j}^{\mathrm{sat}}$ when $|e_{i,j}| > 2\delta_{i,j}$.

If $|e_{i,j}| \leq 2\delta_{i,j}$, it is clear that $|d_i^{(j)} - \hat{w}_{i,j}| \leq 2\delta_{i,j}$. Since the disturbance d_i and its derivatives satisfy Assumption 1, it is obtained that $|\hat{w}_{i,j}| \leq \delta_{i,j}$, which means $\hat{w}_{i,j} = \hat{w}_{i,j}^{\mathrm{sat}}$. Then, the following inequality holds

$$|d_i^{(j)} - \hat{w}_{i,j}^{\mathrm{sat}}| = |d_i^{(j)} - \hat{w}_{i,j}| \leq \varepsilon_{i,j}^{\mathrm{sat}}. \tag{14}$$

Therefore, the value of $|d_i^{(j)} - \hat{w}_{i,j}^{\mathrm{sat}}|$ is less than the saturated error bound $\varepsilon_{i,j}^{\mathrm{sat}}$ whose maximum value is not greater than $2\delta_{i,j}$. This completes the proof. ■

From the above analysis, the saturated bound (13) is able to quantify the impacts caused by estimation error $|d_i^{(j)} - \hat{w}_{i,j}^{\mathrm{sat}}|$. Specially, its transient value is no more than twice the bound of disturbance, and the steady value can be adjusted by choosing the observer parameter matrix $\boldsymbol{L}_i$. In the next section, the saturated estimates $\hat{w}_{i,j}^{\mathrm{sat}}$ will be used to compensate for the impacts to safety caused by the disturbances, and the $\varepsilon_{i,j}^{\mathrm{sat}}$ will be used to quantify the errors between $d_i^{(j)}$ and $\hat{w}_{i,j}^{\mathrm{sat}}$.

Remark *3:* Based on the above analysis, the proposed disturbance observer can accurately estimate a wide range of disturbances with sufficiently small estimation errors. However, it should be highlighted that if the disturbance $\boldsymbol{d}$ can be described by a known exogenous system as proposed in [34], then the estimation error will exponentially converge to zero.

B. Disturbance rejection CBF design

Now, we are able to show the proposed robust safety control approach. Let $\eta_0(\boldsymbol{x}) = b(\boldsymbol{x})$ and define a series of disturbance-dependent auxiliary functions for $\forall i \in \mathbb{N}_{2:r-1}$

$$\begin{aligned}
&\eta_1(\boldsymbol{x}, \boldsymbol{d}) = \big(\frac{\mathrm{d}}{\mathrm{dt}} + p_1\big)\eta_0(\boldsymbol{x}), \\
&\eta_i(\boldsymbol{x}, \boldsymbol{d}, \ldots, \boldsymbol{d}^{(i-1)}) = \big(\frac{\mathrm{d}}{\mathrm{dt}} + p_i\big)\eta_{i-1}(\boldsymbol{x}, \boldsymbol{d}, \ldots, \boldsymbol{d}^{(i-2)}), \\
&\eta_r(\boldsymbol{x}, \boldsymbol{u}, \boldsymbol{d}, \ldots, \boldsymbol{d}^{(r-1)}) = \big(\frac{\mathrm{d}}{\mathrm{dt}} + p_r\big)\eta_{r-1}(\boldsymbol{x}, \boldsymbol{d}, \ldots, \boldsymbol{d}^{(r-2)})
\end{aligned} \tag{15}$$

with positive constants $p_j,\ j \in \mathbb{N}_{1:r}$, and following 0-superlevel sets

$$\boldsymbol{C}_i \triangleq \{(\boldsymbol{x}, \boldsymbol{d}, \ldots, \boldsymbol{d}^{(i-1)}) \in \mathbb{R}^n \times \bar{\mathbb{D}}_{i-1} :\ \eta_i \geq 0, i \in \mathbb{N}_{1:r-1}\}. \tag{16}$$

From (7) and (15), $\eta_i(\boldsymbol{x}, \boldsymbol{d}, \ldots, \boldsymbol{d}^{(i-1)})$ can be expressed as

$$\eta_i(\boldsymbol{x}, \ldots, \boldsymbol{d}^{(i-1)}) = \sum_{j=1}^{i} k_j[\alpha_j(\boldsymbol{x}) + \beta_j(\boldsymbol{x}, \ldots, \boldsymbol{d}^{(i-1)})] + k_0 b(\boldsymbol{x}), \tag{17}$$

where $k_j, j \in \mathbb{N}_{0:i}$ are the parameters of polynomial $k_j s^i + k_{j-1}s^{i-1} + \ldots + k_1 s + k_0$ with negative eigenvalues $-p_1, \ldots, -p_i$. Defining the estimation vectors $\hat{\boldsymbol{d}}_{\mathrm{sat}}^{(i)} = [\hat{w}_{1,i}^{\mathrm{sat}}, \hat{w}_{2,i}^{\mathrm{sat}}, \ldots, \hat{w}_{n,i}^{\mathrm{sat}}]^T$ from (12), it is obtained that

$$\begin{aligned}
\eta_i =& \sum_{j=1}^{i} k_j\alpha_j(\boldsymbol{x}) + \sum_{j=1}^{i} k_j\beta_j(\boldsymbol{x}, \hat{\boldsymbol{d}}_{\mathrm{sat}}, \ldots, \hat{\boldsymbol{d}}_{\mathrm{sat}}^{(j-1)}) + k_0 b(\boldsymbol{x}) \\
&+ \sum_{j=1}^{i} k_j[\beta_j(\boldsymbol{x}, \boldsymbol{d}, \ldots, \boldsymbol{d}^{(j-1)}) - \beta_j(\boldsymbol{x}, \hat{\boldsymbol{d}}_{\mathrm{sat}}, \ldots, \hat{\boldsymbol{d}}_{\mathrm{sat}}^{(j-1)})].
\end{aligned} \tag{18}$$

Define $\boldsymbol{\varpi}_j = [\varepsilon_{1,0}^{\mathrm{sat}}, \ldots, \varepsilon_{1,j-1}^{\mathrm{sat}}, \ldots, \varepsilon_{n,0}^{\mathrm{sat}}, \ldots, \varepsilon_{n,j-1}^{\mathrm{sat}}]^T$. Based on the Theorem 1 and Assumption 2, the following estimates hold

$$\begin{aligned}
\eta_i \geq& \sum_{j=1}^{i} k_j\alpha_j(\boldsymbol{x}) + \sum_{j=1}^{i} k_j\beta_j(\boldsymbol{x}, \hat{\boldsymbol{d}}_{\mathrm{sat}}, \ldots, \hat{\boldsymbol{d}}_{\mathrm{sat}}^{(j-1)}) + k_0 b(\boldsymbol{x}) \\
&- \sum_{j=1}^{i} k_j\gamma_j(\boldsymbol{x})\tilde{\gamma}_j(\boldsymbol{\varpi}_j), \\
=& \eta_i(\boldsymbol{x}, \hat{\boldsymbol{d}}_{\mathrm{sat}}, \ldots, \hat{\boldsymbol{d}}_{\mathrm{sat}}^{(i-1)}) - \mu_i(\boldsymbol{x}, \boldsymbol{\varpi}_1, \ldots, \boldsymbol{\varpi}_i),
\end{aligned} \tag{19}$$

where $\mu_i(\boldsymbol{x}, \boldsymbol{\varpi}_1, \ldots, \boldsymbol{\varpi}_i) = \sum_{j=1}^{i} k_j\gamma_j(\boldsymbol{x})\tilde{\gamma}_j(\boldsymbol{\varpi}_j)$. Then, we can conclude the following disturbance rejection control barrier function.

Definition *3:* Consider the system (4) and the disturbance observers (9) with Assumption 1, and the sets $\boldsymbol{C}_i$ (16). A continuously differentiable function $b : \mathbb{R}^n \to \mathbb{R}$ in (7) is a DRCBF of relative degree r, if there exist positive constants $k_j,\ j \in \mathbb{N}_{1:r}$ defined in (17), subject to

$$\begin{aligned}
\sup_{\boldsymbol{u}\in\mathbb{R}^m} \underbrace{\left\{ \sum_{j=1}^{r} k_j[\alpha_j + \beta_j(\boldsymbol{x}, \ldots, \hat{\boldsymbol{d}}_{\mathrm{sat}}^{(j-1)})] + k_0 b(\boldsymbol{x}) + \beta_u\boldsymbol{u} \right\}}_{\eta_r(\boldsymbol{x}, \boldsymbol{u}, \hat{\boldsymbol{d}}_{\mathrm{sat}}, \ldots, \hat{\boldsymbol{d}}_{\mathrm{sat}}^{(r-1)})} \\
\geq \mu_r(\boldsymbol{x}, \boldsymbol{\varpi}_1, \ldots, \boldsymbol{\varpi}_r),
\end{aligned} \tag{20}$$

for all $(\boldsymbol{x}, \boldsymbol{d}, \ldots, \boldsymbol{d}^{(r-2)}) \in \bar{\boldsymbol{C}} \triangleq \bigcap_{i=0}^{r-1} \boldsymbol{C}_i$.

Theorem *2:* Given a DRCBF and well-designed disturbance observers (9), if the initial values of $\eta_i(\boldsymbol{x}, \hat{\boldsymbol{d}}_{\mathrm{sat}}, \ldots, \hat{\boldsymbol{d}}_{\mathrm{sat}}^{(i-1)}) - \mu_i(\boldsymbol{x}, \boldsymbol{\varpi}_1, \ldots, \boldsymbol{\varpi}_i), i \in \mathbb{N}_{0:r-1}$ are positive, then any Lipschitz

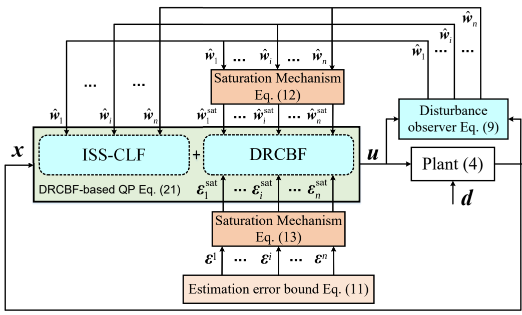

Fig. 2: The control block of the disturbance rejection CBF-based safety-critical control.

continuous controller $\boldsymbol{u}(t,\boldsymbol{x},\hat{\boldsymbol{d}}_{\text{sat}},\ldots,\hat{\boldsymbol{d}}_{\text{sat}}^{(r-1)})\in K_{\text{DRCBF}}\triangleq\{\boldsymbol{u}\in\mathbb{R}^m|\sum_{j=1}^{r}k_j[\alpha_j(\boldsymbol{x})+\beta_j(\boldsymbol{x},\hat{\boldsymbol{d}}_{\text{sat}},\ldots,\hat{\boldsymbol{d}}_{\text{sat}}^{(j-1)})]+k_0b(\boldsymbol{x})+\boldsymbol{\beta}_u(\boldsymbol{x})\boldsymbol{u}\geq\mu_r(\boldsymbol{x},\boldsymbol{\varpi}_1,\ldots,\boldsymbol{\varpi}_r)\}$ renders the set $\bar{\boldsymbol{C}}$ forward invariant for the disturbed system (4).

Proof: First, since $\eta_i(\boldsymbol{x}(0),\hat{\boldsymbol{d}}_{\text{sat}}(0),\ldots,\hat{\boldsymbol{d}}_{\text{sat}}^{(i-1)}(0))-\mu_i(\boldsymbol{x}(0),\boldsymbol{\varpi}_1(0),\ldots,\boldsymbol{\varpi}_i(0)), i\in\mathbb{N}_{1:r-1}$ are positive, it can be obtained from (19) that $\eta_i(\boldsymbol{x}(0),\ldots,\boldsymbol{d}^{(i-1)}(0))\geq 0$, i.e., $[\boldsymbol{x}^T(0),\ldots,\boldsymbol{d}^{(i-1)T}]^T\in\boldsymbol{C}_i$. Since there exists a Lipschitz continuous controller $\boldsymbol{u}(t,\boldsymbol{x},\hat{\boldsymbol{d}}_{\text{sat}},\ldots,\hat{\boldsymbol{d}}_{\text{sat}}^{(r-1)})\in K_{\text{DRCBF}}$, it can be obtained that $\eta_r(\boldsymbol{x},\boldsymbol{u},\ldots,\boldsymbol{d}^{(r-1)})\geq\eta_r(\boldsymbol{x},\boldsymbol{u},\ldots,\hat{\boldsymbol{d}}_{\text{sat}}^{(r-1)})-\mu_r(\boldsymbol{x},\boldsymbol{\varpi}_1,\ldots,\boldsymbol{\varpi}_r)\geq 0$. From (15), we have $\dot{\eta}_{r-1}(\boldsymbol{x}\ldots,\boldsymbol{d}^{(r-2)})=-p_r\eta_{r-1}(\boldsymbol{x},\boldsymbol{d},\ldots,\boldsymbol{d}^{(r-2)})+\eta_r(\boldsymbol{x},\boldsymbol{u},\boldsymbol{d},\ldots,\boldsymbol{d}^{(r-1)})$ such that the set $\boldsymbol{C}_{r-1}$ is forward invariant. Then, the forward invariance of $\boldsymbol{C}_{r-2}$ can also be guaranteed for that of $\boldsymbol{C}_{r-1}$ and $[\boldsymbol{x}^T(0),\boldsymbol{d}^T(0),\ldots,\boldsymbol{d}^{(r-3)T}(0)]^T\in\boldsymbol{C}_{r-2}$. Therefore, following a recursive analysis from the forward invariance of $\boldsymbol{C}_{r-1}$ to that of $\boldsymbol{C}_0$, the forward invariant property of set $\bar{\boldsymbol{C}}$ can be achieved such that the strict safety constraint is guaranteed. This completes the proof. ∎

C. Optimisation-based robust safety control with DRCBF

Based on the results of Theorem 2, the robust safety specification described by $\bar{\boldsymbol{C}}$ can be guaranteed via a Lipschitz continuous controller $\boldsymbol{u}(t,\boldsymbol{x},\hat{\boldsymbol{d}}_{\text{sat}},\ldots,\hat{\boldsymbol{d}}_{\text{sat}}^{(r-1)})\in K_{\text{DRCBF}}$. In order to achieve the safety and stability tasks simultaneously, one possible way is to construct a quadratic programming (QP) by combining the proposed DRCBF and a well-designed CLF for the control task. In this paper, the ISS-CLF proposed in [30] is used. Suppose there is a positive definite function $V:\mathbb{R}^n\to\mathbb{R}_+$ for the control objective of the disturbed system (4), then the following DRCBF-based quadratic program (DRCBF QP) is designed

$$\begin{aligned}&\underset{(\boldsymbol{u},\delta)\in\mathbb{R}^m\times\mathbb{R}}{\arg\min}\ \frac{1}{2}\boldsymbol{u}^T\boldsymbol{u}+\frac{m}{2}\delta^2, \qquad \textbf{DRCBF QP}\\ &\text{s.t. } \varphi_0(\boldsymbol{x},\ldots,\hat{\boldsymbol{d}}_{\text{sat}}^{(r-1)})+\boldsymbol{\varphi}_1(\boldsymbol{x})\boldsymbol{u}-\mu_r(\boldsymbol{x},\ldots,\boldsymbol{\varpi}_r)\geq 0,\\ &\qquad \phi_0(\boldsymbol{x},\hat{\boldsymbol{d}})+\boldsymbol{\phi}_1(\boldsymbol{x})\boldsymbol{u}+\frac{1}{\epsilon}\|\frac{\partial V(\boldsymbol{x})}{\partial\boldsymbol{x}}\|^2\leq -cV+\delta,\end{aligned}\tag{21}$$

where $\varphi_0=\sum_{j=1}^{r}k_j[\alpha_j(\boldsymbol{x})+\beta_j(\boldsymbol{x},\ldots,\hat{\boldsymbol{d}}_{\text{sat}}^{(j-1)})]+k_0b(\boldsymbol{x})$, $\boldsymbol{\varphi}_1=\boldsymbol{\beta}_u(\boldsymbol{x})$, and $\phi_0=L_fV(\boldsymbol{x})+\frac{\partial V(x)}{\partial x}\hat{\boldsymbol{d}}$, $\boldsymbol{\phi}_1=L_gV(\boldsymbol{x})$, c,ϵ are positive constants to be selected. A slack variable δ is introduced to make the above optimisation problem feasible, and $m>0$ is the weight of the cost function to regulate the amplitude of δ. The schematic block of the proposed robust safety-critical control approach is presented in Fig. 2.

In the following, we will show that a Lipschitz continuous controller can be obtained by solving the DRCBF QP.

Theorem *3:* Suppose the functions $\phi_0(\boldsymbol{x},\hat{\boldsymbol{d}})+\frac{1}{\epsilon}\|\frac{\partial V(\boldsymbol{x})}{\partial\boldsymbol{x}}\|^2$, $\boldsymbol{\phi}_1(\boldsymbol{x})$, $\alpha_i(\boldsymbol{x})$, $\beta_i(\boldsymbol{x},\boldsymbol{d},\ldots,\boldsymbol{d}^{(i-1)})$, $\boldsymbol{\beta}_u(\boldsymbol{x})$, $\gamma_i(\boldsymbol{x})$ and $\tilde{\gamma}_i(\boldsymbol{\varpi})$, $i\in\mathbb{N}_{1:r}$ are all locally Lipschitz continuous in state $\boldsymbol{x}$ and continuous in t. Then, the solution of DRCBF-QP is locally Lipschitz continuous in $\boldsymbol{x}$ and continuous in t.

The Lipschitz continuity analysis can be discussed following the results in [5], [13]. For the sake of completeness of this paper, the proof is given in the Appendix.

IV. Application to Path Following of UAV with Wind Disturbances

In this section, we consider a surveillance task for UAV within a specified safety region, which demands close-range observation of an interesting area and collision avoidance from the region borders. To this end, a periodic patrol path is designed as the desired path, which is given by

$$p_x^c(\theta)=10\theta-220,\ p_y^c(\theta)=-50\sin(0.25\theta),\tag{22}$$

where $\theta\in[\underline{\theta},\bar{\theta}]$ is the path parameter, and $\underline{\theta},\bar{\theta}$ represent its minimum and maximum, respectively. By augmenting a virtual control u_θ to adjust the dynamics of path parameter θ, it is obtained that

$$\begin{aligned}&\dot{p}_x=V_a\cos\psi+d_x,\ \dot{p}_y=V_a\sin\psi+d_y,\ \dot{\psi}=u_\psi,\\&\dot{\theta}_1=\theta_2,\ \dot{\theta}_2=u_\theta,\end{aligned}\tag{23}$$

where $\theta_1=\theta$ and $\theta_2=\dot{\theta}$. We assume there exist known positive constants $\delta_{i,0}$, $\delta_{i,1}$ and $\delta_{i,2}$ satisfying $|d_i(t)|\leq\delta_{i,0}$, $|\dot{d}_i(t)|\leq\delta_{i,1}$ and $|\ddot{d}_i(t)|\leq\delta_{i,2}$, $i=\{x,y\}$. Based on the disturbance observer (9), the following disturbance observers are constructed

$$\begin{aligned}\dot{\xi}_{x,0}&=\xi_{x,1}+l_2p_x-l_1(V_a\cos\psi+\xi_{x,0}+l_1p_x),\\\dot{\xi}_{x,1}&=-l_2(V_a\cos\psi+\xi_{x,0}+l_1p_x),\\\dot{\xi}_{y,0}&=\xi_{y,1}+l_2p_y-l_1(V_a\sin\psi+\xi_{y,0}+l_1p_y),\\\dot{\xi}_{y,1}&=-l_2(V_a\sin\psi+\xi_{y,0}+l_1p_y),\end{aligned}\tag{24}$$

where $\hat{w}_{x,0}=\xi_{x,0}+l_1p_x,\hat{w}_{y,0}=\xi_{y,0}+l_1p_y,\hat{w}_{x,1}=\xi_{x,1}+l_2p_x,\hat{w}_{y,1}=\xi_{y,1}+l_2p_y$ are the winds and their derivative estimates, and l_1,l_2 are observer parameters to be designed. Following the proposed estimation error quantification mechanism (12) and (13), we denote $\hat{w}_{x,0}^{\text{sat}},\hat{w}_{y,0}^{\text{sat}},\hat{w}_{x,1}^{\text{sat}},\hat{w}_{y,1}^{\text{sat}}$ and $\varepsilon_{x,0}^{\text{sat}},\varepsilon_{y,0}^{\text{sat}},\varepsilon_{x,1}^{\text{sat}},\varepsilon_{y,1}^{\text{sat}}$ as the saturated estimates and proposed error bounds, respectively.

A. ISS-CLF-based path following controller design

Defining the path following errors as $z_1=p_x-p_x^c$, $z_2=V_a\cos\psi-\frac{\partial p_x^c}{\partial\theta}\theta_2$, $z_3=p_y-p_y^c$ and $z_4=V_a\sin\psi-\frac{\partial p_y^c}{\partial\theta}\theta_2$, the tracking error dynamics is expressed as follows

$$\begin{aligned}\dot{z}_1&=z_2+d_x,\\\dot{z}_2&=-V_a\sin\psi u_\psi-\frac{\partial p_x^c}{\partial\theta}u_\theta-\frac{\partial^2p_x^c}{\partial\theta^2}\theta_2^2+\dot{d}_x,\\\dot{z}_3&=z_4+d_y,\\\dot{z}_4&=V_a\cos\psi u_\psi-\frac{\partial p_y^c}{\partial\theta}u_\theta-\frac{\partial^2p_y^c}{\partial\theta^2}\theta_2^2+\dot{d}_y.\end{aligned}\tag{25}$$

With the help of disturbance estimates, we define $\hat{\boldsymbol{Z}}=[z_1,\ z_2+\hat{w}_{x,0},\ z_3,\ z_4+\hat{w}_{y,0}]^T$, then it is obtained that

$$\dot{\hat{\boldsymbol{Z}}}=\boldsymbol{A}\hat{\boldsymbol{Z}}+\hat{\boldsymbol{F}}+\boldsymbol{F}_\varepsilon+\boldsymbol{B}\boldsymbol{G}\boldsymbol{v},\tag{26}$$

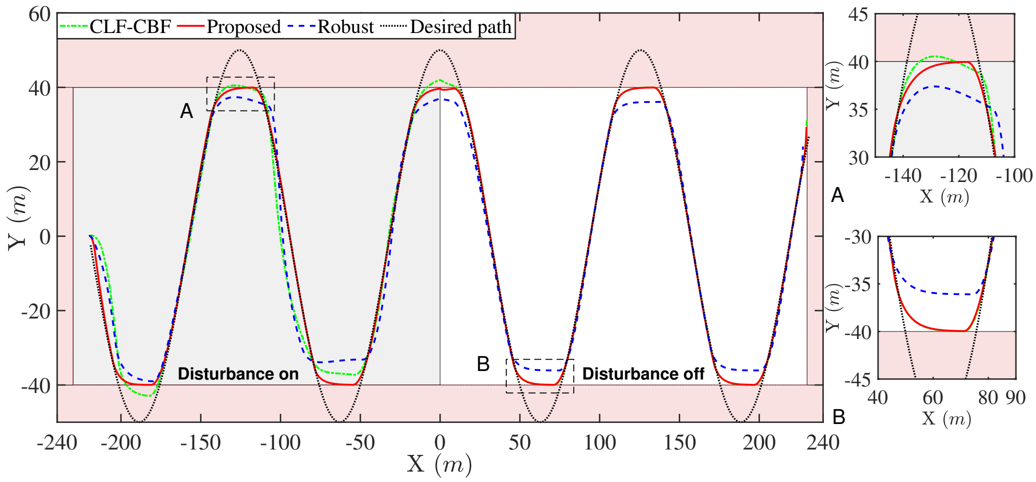

Fig. 3: Path profiles of UAV under the baseline, the DRCBF and the robust path following controllers in the presence of wind disturbances.

with

$$\boldsymbol{A}=\begin{bmatrix}0&1&0&0\\0&0&0&0\\0&0&0&1\\0&0&0&0\end{bmatrix},\boldsymbol{B}=\begin{bmatrix}0&0\\1&0\\0&0\\0&1\end{bmatrix},\boldsymbol{G}=\begin{bmatrix}-V_a\sin\psi & -\frac{\partial p_x^c}{\partial\theta}\\ V_a\cos\psi & -\frac{\partial p_y^c}{\partial\theta}\end{bmatrix}, \tag{27}$$

where $\boldsymbol{v}=[u_\psi,u_\theta]^T$, $\hat{\boldsymbol{F}}=[0,-\frac{\partial^2 p_x^c}{\partial\theta^2}\theta_2^2+\hat{w}_{x,1},0,-\frac{\partial^2 p_x^c}{\partial\theta^2}\theta_2^2+\hat{w}_{y,1}]^T$ and $\boldsymbol{F}_\varepsilon=[\varepsilon_{x,0},l_1\varepsilon_{x,0},\varepsilon_{y,0},l_1\varepsilon_{y,0}]^T$ is the estimation error vector.

Based on the works in [30], [35], we can define $V=\hat{\boldsymbol{Z}}^T\boldsymbol{P}\hat{\boldsymbol{Z}}$ as the ISS-CLF for error system (26), where the symmetric positive definite matrix $\boldsymbol{P}$ can be determined by solving the Riccati equation $\boldsymbol{A}^T\boldsymbol{P}+\boldsymbol{P}\boldsymbol{A}-2\boldsymbol{P}\boldsymbol{B}\boldsymbol{B}^T\boldsymbol{P}+\boldsymbol{Q}=0$ with a positive definite matrix $\boldsymbol{Q}$. Then, the path following controller with disturbance estimates is formulated as the following quadratic programming

$$\begin{aligned}&\underset{\boldsymbol{v}\in\mathbb{R}^2}{\arg\min}\ \frac{1}{2}\boldsymbol{v}^T\boldsymbol{v}, && \textbf{Path following QP}\\ &\text{s.t.}\quad \phi_0(\hat{\boldsymbol{Z}},\hat{\boldsymbol{w}}_x,\hat{\boldsymbol{w}}_y)+\boldsymbol{\phi}_1(\hat{\boldsymbol{Z}})\boldsymbol{v}+\frac{1}{\epsilon}\|2\hat{\boldsymbol{Z}}^T\boldsymbol{P}\|^2\le -cV,\end{aligned} \tag{28}$$

where $\phi_0(\hat{\boldsymbol{Z}},\hat{\boldsymbol{w}}_x,\hat{\boldsymbol{w}}_y)=\hat{\boldsymbol{Z}}^T(\boldsymbol{A}^T\boldsymbol{P}+\boldsymbol{P}\boldsymbol{A})\hat{\boldsymbol{Z}}+2\hat{\boldsymbol{Z}}^T\boldsymbol{P}\hat{\boldsymbol{F}}$ and $\boldsymbol{\phi}_1(\hat{\boldsymbol{Z}})=2\hat{\boldsymbol{Z}}^T\boldsymbol{P}\boldsymbol{B}\boldsymbol{G}$, and $\hat{\boldsymbol{w}}_x=[\hat{w}_{x,0},\ \hat{w}_{x,1}]^T$, $\hat{\boldsymbol{w}}_y=[\hat{w}_{y,0},\ \hat{w}_{y,1}]^T$.

B. Safety-critical path following controller design

In this scenario, the safety region is considered as $-x_b\le x\le x_b$ and $-y_b\le y\le y_b$ with $x_b=230$, $y_b=40$, and the collision avoidance specifications are interpreted by the following two pair sharing control barrier functions [6] as $b_{x,1}(p_x)=x_b+p_x$, $b_{x,2}(p_x)=x_b-p_x$, $b_{y,1}(p_y)=y_b+p_y$ and $b_{y,2}(p_y)=y_b-p_y$. Based on the proposed DRCBF in (21) and the ISS-CLF-based controller in (28), the proposed robust safety-critical path following controller is formulated as the following QP problem

$$\begin{aligned}&\underset{(\boldsymbol{v},\delta)\in\mathbb{R}^2\times\mathbb{R}}{\arg\min}\ \frac{1}{2}\boldsymbol{v}^T\boldsymbol{v}+\frac{m}{2}\delta^2, && \textbf{DRCBF Path Following}\\ &\text{s.t.}\quad \varphi_{x,i}^0(\psi,\hat{\boldsymbol{w}}_x^{\text{sat}})+\boldsymbol{\varphi}_{x,i}^1(\psi)\boldsymbol{v}-\mu_x(\boldsymbol{\varepsilon}_x^{\text{sat}})\ge 0,\\ &\qquad \varphi_{y,i}^0(\psi,\hat{\boldsymbol{w}}_y^{\text{sat}})+\boldsymbol{\varphi}_{y,i}^1(\psi)\boldsymbol{v}-\mu_y(\boldsymbol{\varepsilon}_y^{\text{sat}})\ge 0,\ i\in\mathbb{N}_{1:2}\\ &\qquad \phi_0(\hat{\boldsymbol{Z}},\hat{\boldsymbol{w}}_x,\hat{\boldsymbol{w}}_y)+\boldsymbol{\phi}_1(\hat{\boldsymbol{Z}})\boldsymbol{v}+\frac{1}{\epsilon}\|2\hat{\boldsymbol{Z}}^T\boldsymbol{P}\|^2\le -cV+\delta,\end{aligned} \tag{29}$$

with

$$\begin{aligned}\varphi_{x,1}^0 &=k_1V_a\cos\psi+k_0b_{x,1}+k_1\hat{w}_{x,0}^{\text{sat}}+\hat{w}_{x,1}^{\text{sat}},\\ \varphi_{x,2}^0 &=-k_1V_a\cos\psi+k_0b_{x,2}-k_1\hat{w}_{x,0}^{\text{sat}}-\hat{w}_{x,1}^{\text{sat}},\\ \varphi_{y,1}^0 &=k_1V_a\sin\psi+k_0b_{y,1}+k_1\hat{w}_{y,0}^{\text{sat}}+\hat{w}_{y,1}^{\text{sat}},\\ \varphi_{y,2}^0 &=-k_1V_a\sin\psi+k_0b_{y,2}-k_1\hat{w}_{y,0}^{\text{sat}}-\hat{w}_{y,1}^{\text{sat}},\\ \mu_x &=k_1\varepsilon_{x,0}^{\text{sat}}+\varepsilon_{x,1}^{\text{sat}},\ \mu_y=k_1\varepsilon_{y,0}^{\text{sat}}+\varepsilon_{y,1}^{\text{sat}},\end{aligned} \tag{30}$$

where $\boldsymbol{\varepsilon}_x^{\text{sat}}=[\varepsilon_{x,0}^{\text{sat}},\ \varepsilon_{x,1}^{\text{sat}}]^T$, $\boldsymbol{\varepsilon}_y^{\text{sat}}=[\varepsilon_{y,0}^{\text{sat}},\ \varepsilon_{y,1}^{\text{sat}}]^T$, $\boldsymbol{\varphi}_{x,1}^1=[-V_a\sin\psi,0]$, $\boldsymbol{\varphi}_{x,2}^1=-\boldsymbol{\varphi}_{x,1}^1$, $\boldsymbol{\varphi}_{y,1}^1=[V_a\cos\psi,0]$, $\boldsymbol{\varphi}_{y,2}^1=\boldsymbol{\varphi}_{y,1}^1$ and k_0,k_1 are parameters to be designed for the DRCBF.

C. Simulation results

The initial states of UAV are $p_x(0)=-220$m, $p_y(0)=0$m, $\psi(0)=-\frac{\pi}{60}$rad, and the initial conditions of θ are $\theta(0)=\frac{\pi}{16}$, $\dot{\theta}(0)=0.1$. The airspeed of UAV is $V_a=15$m/s. The external winds d_x and d_y are set as $d_x=3.5\cos(0.5t)$m/s and $d_y=6\cos(0.5t)$m/s. The observer parameters are set as $l_1=100$, $l_2=2400$ and the bounds of external wind disturbances are assumed as $\delta_{x,0}=4$, $\delta_{y,0}=7$, $\delta_{x,1}=3$, $\delta_{y,1}=4.5$ and $\delta_{x,2}=2$, $\delta_{y,2}=3$. The disturbances are introduced to the system at the start and removed once $x(t)\ge 0$. The control parameters are selected as $\boldsymbol{Q}=\text{diag}([4,1,1,1]^{\text{T}})$, $\epsilon=1$, $c=5$, $m=0.01$ and $k_0=16$, $k_1=8$.

In the following, to further exhibit its safety robustness against unmatched disturbances and the feature of performance recovery, the proposed controller is compared with the baseline CLF-CBF-based controller without disturbance consideration proposed in [5] and the robust CLF-CBF-based one using the conservative overapproximate bounds of external disturbances proposed in [14]. The robust safety controller with worst-case disturbances is designed as follows

$$\begin{aligned}&\underset{(v,\delta)\in\mathbb{R}^2\times\mathbb{R}}{\arg\min}\ \frac{1}{2}\boldsymbol{v}^T\boldsymbol{v}+\frac{m}{2}\delta^2, && \textbf{Robust Path Following}\\ &\text{s.t.}\quad \bar{\varphi}_{x,i}^0(\psi)+\boldsymbol{\varphi}_{x,i}^1(\psi)\boldsymbol{v}-\varsigma_x(\psi,\delta_{x,0},\delta_{x,1})\ge 0,\\ &\qquad \bar{\varphi}_{y,i}^0(\psi)+\boldsymbol{\varphi}_{y,i}^1(\psi)\boldsymbol{v}-\varsigma_y(\psi,\delta_{y,0},\delta_{y,1})\ge 0,\ i\in\mathbb{N}_{1:2}\\ &\qquad \psi_0(\boldsymbol{Z})+\boldsymbol{\psi}_1(\boldsymbol{Z})\boldsymbol{v}+|2\boldsymbol{Z}^T\boldsymbol{P}\boldsymbol{F}_\delta|\le -cV+\delta,\end{aligned} \tag{31}$$

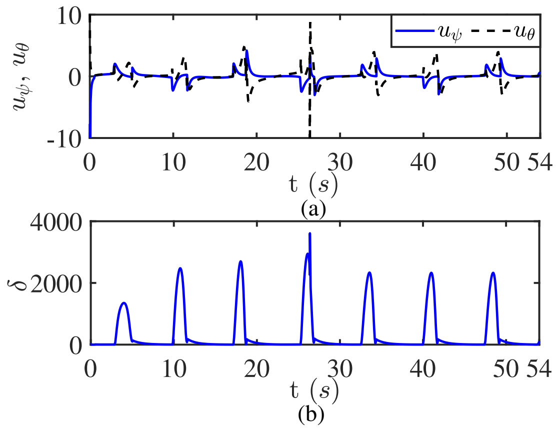

Fig. 4: Control input curves of UAV under DRCBF path following controller: (a) control inputs u_θ and u_ψ; (b) slack variable δ.

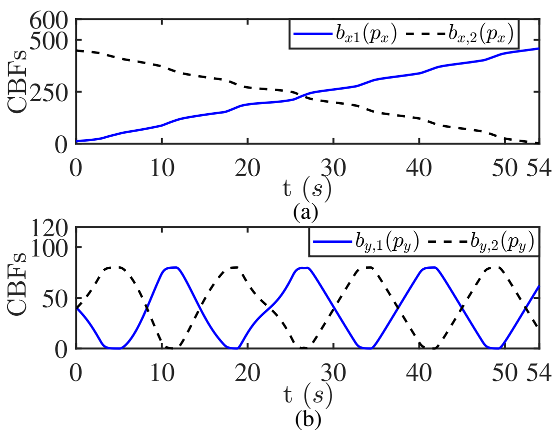

Fig. 5: Trajectories of CBFs under DRCBF path following controller: (a) CBFs in X axis; (b) CBFs in Y axis.

with

$$
\begin{aligned}
\bar{\varphi}^0_{x,1} =& k_1 V_a \cos\psi + k_0 b_{x,1},\ \bar{\varphi}^0_{x,2} = -k_1 V_a \cos\psi + k_0 b_{x,2},\\
\bar{\varphi}^0_{y,1} =& k_1 V_a \sin\psi + k_0 b_{y,1},\ \bar{\varphi}^0_{y,2} = -k_1 V_a \sin\psi + k_0 b_{y,2},\\
\varsigma_x =& k_1\delta_{x,0} + \delta_{x,1},\ \varsigma_y = k_1\delta_{y,0} + \delta_{y,1},\\
\psi_0 =& \boldsymbol{Z}^T(\boldsymbol{A}^T\boldsymbol{P} + \boldsymbol{P}\boldsymbol{A})\boldsymbol{Z} + 2\boldsymbol{Z}^T\boldsymbol{P}\boldsymbol{F},
\end{aligned}
\tag{32}
$$

where $\boldsymbol{Z} = [z_1, z_2, z_3, z_4]^T$, $\boldsymbol{F} = [0, -\frac{\partial^2 p^c_x}{\partial\theta^2}\theta_2^2, 0, -\frac{\partial^2 p^c_x}{\partial\theta^2}\theta_2^2]^T$, $\boldsymbol{\psi}_1(\boldsymbol{Z}) = 2\boldsymbol{Z}^T\boldsymbol{P}\boldsymbol{B}\boldsymbol{G}$ and $\boldsymbol{F}_\delta = [\delta_{x,0}, \delta_{x,1}, \delta_{y,0}, \delta_{y,1}]^T$.

The path following results under different controllers are shown in Fig. 3, where we present the path following performances in the horizontal plane with wind disturbances. It can be seen that the baseline controller can not prevent UAV from crossing the safety boundary when there exists external wind disturbances. It is worth pointing out that the proposed approach achieves a strict safety guarantee as well as the nominal control performance, regardless of the presence of disturbances. In contrast, the robust approach results in overly conservative safety performances as the UAV is approaching the boundary due to the use of worst-case disturbances. In Fig. 4, the trajectories of control inputs u_ψ, u_θ and slack variable δ are shown, where the slack variable keeps in a relatively small value when there is no conflict between the safety and stability tasks. The trajectories of $b_{x_i}(p_x)$ and $b_{y_i}(p_y)$ presented in Fig. 5 indicate that the safety specifications are achieved. Meanwhile, the disturbances and their estimates are shown in Fig. 6, which demonstrates that the proposed error quantification mechanism achieves accurate and less

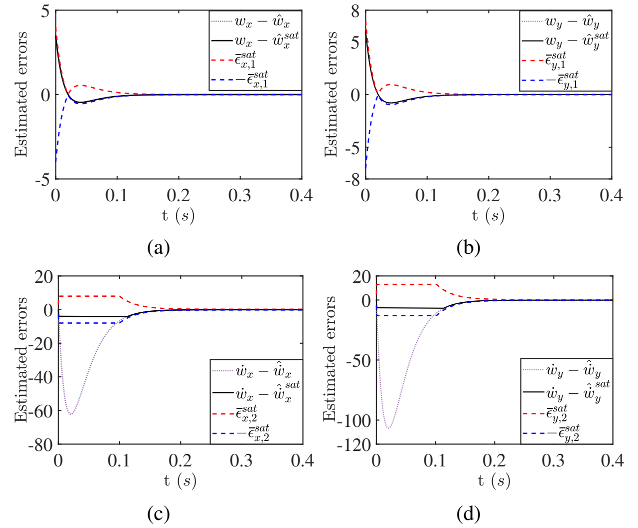

Fig. 6: Estimation error quantification performance of the wind disturbances: (a) estimation errors of w_x;(b) estimation errors of w_y;(c) estimation errors of $\dot{w}_x$;(d) estimation errors of $\dot{w}_y$.

conservative over-estimation performances.

V. Conclusions

In this paper, inspired by the collision avoidance path following of UAV with wind disturbances, where the winds directly impact the dynamics of CBF from the different channels of control input, a disturbance observer-based DRCBF has been developed for a class of nonlinear systems with unmatched disturbances. To achieve strict safety specifications and satisfactory control performances under unmatched disturbances, an optimisation-based control scheme has been proposed based on the techniques of DRCBF and ISS-CLF. It has been demonstrated via the path following of UAV that the proposed method achieves the prescribed safety specification without sacrificing the nominal control performances.

Appendix

Proof: We first consider the solution of the proposed optimisation program. The Lagrangian function of DRCBF QP is illustrated as follows

$$
\begin{aligned}
\mathcal{L} =& \frac{1}{2}\boldsymbol{u}^T\boldsymbol{u} + \frac{m}{2}\delta^2 + \lambda_1[\boldsymbol{a}_1(\boldsymbol{x})\boldsymbol{u} + b_1(\boldsymbol{x}, \hat{\boldsymbol{d}}_{\text{sat}}, \dots, \hat{\boldsymbol{d}}^{(r-1)}_{\text{sat}},\\
& \boldsymbol{\varpi_1}, \dots, \boldsymbol{\varpi_r})] + \lambda_2[\boldsymbol{a}_2(\boldsymbol{x})\boldsymbol{u} - \delta + b_2(\boldsymbol{x}, \hat{\boldsymbol{d}})],
\end{aligned}
\tag{33}
$$

where $\boldsymbol{a}_1(\boldsymbol{x}) = -\boldsymbol{\varphi}_1(\boldsymbol{x})$, $b_1(\boldsymbol{x}, \dots, \hat{\boldsymbol{d}}^{(r-1)}_{\text{sat}}, \dots, \boldsymbol{\varpi_r}) = -\varphi_0(\boldsymbol{x}, \hat{\boldsymbol{d}}_{\text{sat}}, \dots, \hat{\boldsymbol{d}}^{(r-1)}_{\text{sat}}) + \mu_r(\boldsymbol{x}, \boldsymbol{\varpi_1}, \dots, \boldsymbol{\varpi_r})$, $\boldsymbol{a}_2(\boldsymbol{x}) = \boldsymbol{\phi}_1(\boldsymbol{x})$, $b_2(\boldsymbol{x}, \hat{\boldsymbol{d}}) = \phi_0(\boldsymbol{x}, \hat{\boldsymbol{d}}) + \frac{1}{\epsilon}\|\frac{\partial V(\boldsymbol{x})}{\partial \boldsymbol{x}}\|^2 + cV(\boldsymbol{x})$, and $\lambda_i, i = \{1, 2\}$ are scalar Lagrange multipliers. For brevity, the arguments of $\boldsymbol{a}_i, b_i,\ i \in \mathbb{N}_{1:2}$ are omitted. By applying the Karush-Kuhn-Tucker (KKT) condition in [36], the explicit control laws can be obtained under four cases where different constraints are active.

Case 1: Both the safety and stability constraints are inactive ($\lambda_1 = 0,\ \lambda_2 = 0$). Then, the solution of the optimisation program is given by

$$
\boldsymbol{u} = \boldsymbol{0},\ \delta = 0. \tag{34}
$$

The region in which the above solution applies is $\Omega_1 := \{(t, \boldsymbol{x}, \hat{\boldsymbol{d}}, \hat{\boldsymbol{d}}_{\text{sat}}, \dots, \hat{\boldsymbol{d}}^{(r-1)}_{\text{sat}}) \in \mathbb{R}_+ \times X \times \mathbb{R}^n \times \bar{\mathbb{D}}_{r-1} :\ b_1 \leq 0, b_2 \leq 0\}$.

Case 2: Only the safety constraint is active ($\lambda_1 \geq 0$, $\lambda_2 = 0$), and the solution is given by

$$\boldsymbol{u} = -\frac{b_1}{\|\boldsymbol{a}_1\|^2}\boldsymbol{a}_1^T, \ \delta = 0, \tag{35}$$

where the solution applies is $\Omega_2 := \{(t, \boldsymbol{x}, \hat{\boldsymbol{d}}, \hat{\boldsymbol{d}}_{\rm sat}, \ldots, \hat{\boldsymbol{d}}_{\rm sat}^{(r-1)}) \in \mathbb{R}_+ \times X \times \mathbb{R}^n \times \bar{\mathbb{D}}_{r-1} : \ b_1 \geq 0, b_2 \leq \frac{\boldsymbol{a}_2 b_1}{\|\boldsymbol{a}_1\|^2}\boldsymbol{a}_1^T\}$.

Case 3: Only the stability constraint is active, while the safety constraint is inactive ($\lambda_1 = 0$, $\lambda_2 \geq 0$). The relative optimal solution is

$$\boldsymbol{u} = -\frac{mb_2}{1 + m\|\boldsymbol{a}_2\|^2}\boldsymbol{a}_2^T, \ \delta = \frac{b_2}{1 + m\|\boldsymbol{a}_2\|^2}. \tag{36}$$

The above solution holds in $\Omega_3 := \{(t, \boldsymbol{x}, \hat{\boldsymbol{d}}, \hat{\boldsymbol{d}}_{\rm sat}, \ldots, \hat{\boldsymbol{d}}_{\rm sat}^{(r-1)}) \in \mathbb{R}_+ \times X \times \mathbb{R}^n \times \bar{\mathbb{D}}_{r-1} : \ b_1 \leq \frac{m\boldsymbol{a}_1 b_2}{1+m\|\boldsymbol{a}_2\|^2}\boldsymbol{a}_2^T, b_2 \geq 0\}$.

Case 4: Both the safety and stability constraints are active ($\lambda_1 \geq 0$, $\lambda_2 \geq 0$), and we can obtain the following solution

$$\begin{aligned}\boldsymbol{u} =& \frac{-[(\|\boldsymbol{a}_2\|^2 + 1/m)b_1 - \boldsymbol{a}_1\boldsymbol{a}_2^T b_2]\boldsymbol{a}_1^T - (\|\boldsymbol{a}_1\|^2 b_2 - \boldsymbol{a}_2\boldsymbol{a}_1^T b_1)\boldsymbol{a}_2^T}{\|\boldsymbol{a}_1\|^2(\|\boldsymbol{a}_2\|^2 + 1/m) - \|\boldsymbol{a}_1\boldsymbol{a}_2^T\|^2} \\ \delta =& \frac{\|\boldsymbol{a}_1\|^2 b_2 - \boldsymbol{a}_2\boldsymbol{a}_1^T b_1}{m\|\boldsymbol{a}_1\|^2(\|\boldsymbol{a}_2\|^2 + 1/m) - m\|\boldsymbol{a}_1\boldsymbol{a}_2^T\|^2},\end{aligned} \tag{37}$$

where the solution applies is $\Omega_4 := \{(t, \boldsymbol{x}, \hat{\boldsymbol{d}}, \hat{\boldsymbol{d}}_{\rm sat}, \ldots, \hat{\boldsymbol{d}}_{\rm sat}^{(r-1)}) \in \mathbb{R}_+ \times X \times \mathbb{R}^n \times \bar{\mathbb{D}}_{r-1} : \ b_2 \geq \frac{\boldsymbol{a}_2 b_1}{\|\boldsymbol{a}_1\|^2}\boldsymbol{a}_1^T, b_1 \geq \frac{\boldsymbol{a}_1 b_2}{\|\boldsymbol{a}_2\|^2 + 1/m}\boldsymbol{a}_2^T, b_1 > 0, b_2 > 0\}$.

It can be verified that the functions $\boldsymbol{a}_0$, $\boldsymbol{a}_1$, $\boldsymbol{b}_1$ and $\boldsymbol{b}_2$ are all locally Lipschitz continuous functions $\boldsymbol{x}$ and continuous in t, since the functions $\phi_0 + \frac{1}{\epsilon}\|\frac{\partial V(\boldsymbol{x})}{\partial \boldsymbol{x}}\|^2$, $\boldsymbol{\phi}_1$, α_i, $\boldsymbol{\beta}_u$, γ_i and $\tilde{\gamma}_i$ are all locally Lipschitz continuous in state $\boldsymbol{x}$ and continuous in t. Due to the fact that $\boldsymbol{\beta}_u(\boldsymbol{x}) \neq 0$, then following a similar analysis proceed in [5], [13], the proposed control law is locally Lipschitz continuous in $\boldsymbol{x}$ and continuous in t. This completes the proof. ■

References

[1] U. Ozguner, C. Stiller, and K. Redmill, "Systems for safety and autonomous behavior in cars: The darpa grand challenge experience," *Proceedings of the IEEE*, vol. 95, no. 2, pp. 397–412, 2007.

[2] A. D. Ames, J. W. Grizzle, and P. Tabuada, "Control barrier function based quadratic programs with application to adaptive cruise control," in *Proceedings of the IEEE Conference on Decision and Control (CDC)*, 2014, pp. 6271–6278.

[3] L. Wang, A. D. Ames, and M. Egerstedt, "Safety barrier certificates for collisions-free multirobot systems," *IEEE Transactions on Robotics*, vol. 33, no. 3, pp. 661–674, 2017.

[4] A. M. Zanchettin, N. M. Ceriani, P. Rocco, H. Ding, and B. Matthias, "Safety in human-robot collaborative manufacturing environments: Metrics and control," *IEEE Transactions on Automation Science and Engineering*, vol. 13, no. 2, pp. 882–893, 2015.

[5] A. D. Ames, X. Xu, J. W. Grizzle, and P. Tabuada, "Control barrier function based quadratic programs for safety critical systems," *IEEE Transactions on Automatic Control*, vol. 62, no. 8, pp. 3861–3876, 2017.

[6] X. Xu, "Constrained control of input-output linearizable systems using control sharing barrier functions," *Automatica*, vol. 87, pp. 195–201, 2018.

[7] M. Jankovic, "Robust control barrier functions for constrained stabilization of nonlinear systems," *Automatica*, vol. 96, pp. 359–367, 2018.

[8] W. Xiao and C. Belta, "High order control barrier functions," *IEEE Transactions on Automatic Control*, vol. 67, no. 7, pp. 3655–3662, 2021.

[9] S.-C. Hsu, X. Xu, and A. D. Ames, "Control barrier function based quadratic programs with application to bipedal robotic walking," in *Proceedings of the American Control Conference (ACC)*, 2015, pp. 4542–4548.

[10] A. D. Ames, S. Coogan, M. Egerstedt, and et al., "Control barrier functions: Theory and applications," in *Proceedings of the European Control Conference (ECC)*, 2019, pp. 3420–3431.

[11] W. Xiao, C. G. Cassandras, and C. A. Belta, "Bridging the gap between optimal trajectory planning and safety-critical control with applications to autonomous vehicles," *Automatica*, vol. 129, p. 109592, 2021.

[12] Q. Nguyen and K. Sreenath, "Exponential control barrier functions for enforcing high relative-degree safety-critical constraints," in *Proceedings of the American Control Conference (ACC)*, 2016, pp. 322–328.

[13] X. Xu, P. Tabuada, J. W. Grizzle, and A. D. Ames, "Robustness of control barrier functions for safety critical control," *IFAC-PapersOnLine*, vol. 48, no. 27, pp. 54–61, 2015.

[14] Q. Nguyen and K. Sreenath, "Robust safety-critical control for dynamic robotics," *IEEE Transactions on Automatic Control*, vol. 67, no. 3, pp. 1073–1088, 2021.

[15] E. D. Sontag and Y. Wang, "On characterizations of the input-to-state stability property," *Systems & Control Letters*, vol. 24, no. 5, pp. 351–359, 1995.

[16] A. Alan, A. J. Taylor, C. R. He, G. Orosz, and A. D. Ames, "Safe controller synthesis with tunable input-to-state safe control barrier functions," *IEEE Control Systems Letters*, vol. 6, pp. 908–913, 2021.

[17] W.-H. Chen, D. J. Ballance, P. J. Gawthrop, and J. O'Reilly, "A nonlinear disturbance observer for robotic manipulators," *IEEE Transactions on Industrial Electronics*, vol. 47, no. 4, pp. 932–938, 2000.

[18] W.-H. Chen, J. Yang, L. Guo, and S. Li, "Disturbance-observer-based control and related methods—An overview," *IEEE Transactions on industrial electronics*, vol. 63, no. 2, pp. 1083–1095, 2015.

[19] E. Daş and R. M. Murray, "Robust safe control synthesis with disturbance observer-based control barrier functions," in *Proceedings of the Conference on Decision and Control (CDC)*. IEEE, 2022, pp. 5566–5573.

[20] A. Alan, T. G. Molnar, E. Das, A. D. Ames, and G. Orosz, "Disturbance observers for robust safety-critical control with control barrier functions," *IEEE Control Systems Letters*, vol. 7, pp. 1123–1128, 2022.

[21] J. Sun, J. Yang, and Z. Zeng, "Safety-critical control with control barrier function based on disturbance observer," *IEEE Transactions on Automatic Control*, vol. 69, no. 7, pp. 4750–4756, 2024.

[22] J. Chen, Z. Gao, and Q. Lin, "Robust control barrier functions for safe control under uncertainty using extended state observer and output measurement," in *Proceedings of the IEEE Conference on Decision and Control (CDC)*. IEEE, 2023, pp. 8477–8482.

[23] V. Hamdipoor, N. Meskin, and C. G. Cassandras, "Safe control synthesis using environmentally robust control barrier functions," *European Journal of Control*, vol. 74, p. 100840, 2023.

[24] S. Li, J. Yang, W.-H. Chen, and X. Chen, "Generalized extended state observer based control for systems with mismatched uncertainties," *IEEE Transactions on Industrial Electronics*, vol. 59, no. 12, pp. 4792–4802, 2011.

[25] J. Yang, W.-H. Chen, and S. Li, "Nonlinear disturbance observer-based robust control for systems with mismatched disturbances/uncertainties," *IET Control Theory & Applications*, vol. 5, no. 18, pp. 2053–2062, 2011.

[26] J. Yang, C. Liu, M. Coombes, Y. Yan, and W.-H. Chen, "Optimal path following for small fixed-wing uavs under wind disturbances," *IEEE Transactions on Control Systems Technology*, vol. 29, no. 3, pp. 996–1008, 2020.

[27] R. Takano and M. Yamakita, "Robust control barrier function for systems affected by a class of mismatched disturbances," *SICE Journal of Control, Measurement, and System Integration*, vol. 13, no. 4, pp. 165–172, 2020.

[28] E. Das and J. W. Burdick, "Robust control barrier functions using uncertainty estimation with application to mobile robots," *arXiv preprint arXiv:2401.01881*, 2024.

[29] Y. Wang and X. Xu, "Disturbance observer-based robust control barrier functions," in *Proceedings of the American Control Conference (ACC)*. IEEE, 2023, pp. 3681–3687.

[30] M. H. Cohen and C. Belta, "Modular adaptive safety-critical control," in *Proceedings of the American Control Conference (ACC)*. IEEE, 2023, pp. 2969–2974.

[31] A. Isidori, *Nonlinear control systems Third Edition*. Springer, 1995.

[32] M. Krstic, "Inverse optimal safety filters," *IEEE Transactions on Automatic Control*, vol. 69, no. 1, pp. 16–31, 2024.

[33] R. W. Beard and T. W. McLain, *Small unmanned aircraft: Theory and practice*. Princeton University Press, 2012.

[34] L. Guo and W.-H. Chen, "Disturbance attenuation and rejection for systems with nonlinearity via DOBC approach," *International Journal of Robust and Nonlinear Control*, vol. 15, no. 3, pp. 109–125, 2005.

[35] A. D. Ames, K. Galloway, K. Sreenath, and J. W. Grizzle, "Rapidly exponentially stabilizing control Lyapunov functions and hybrid zero dynamics," *IEEE Transactions on Automatic Control*, vol. 59, no. 4, pp. 876–891, 2014.

[36] S. Boyd, S. P. Boyd, and L. Vandenberghe, *Convex optimization*. Cambridge University Press, 2004.